IOPscience iopscience.iop.org

Home Search Collections Journals About Contact us My IOPscience

The diffusion of protons in the superionic conductor $CsHSO_4$ by quasielastic neutron scattering

This article has been downloaded from IOPscience. Please scroll down to see the full text article.

1992 J. Phys.: Condens. Matter 4 389

(http://iopscience.iop.org/0953-8984/4/2/008)

View the table of contents for this issue, or go to the journal homepage for more

Download details:
IP Address: 171.66.16.159
The article was downloaded on 12/05/2010 at 11:03

Please note that terms and conditions apply.

J. Phys.: Condens. Matter 4 (1992) 389–398. Printed in the UK

The diffusion of protons in the superionic conductor $CsHSO_4$ by quasielastic neutron scattering

A V Belushkin†, C J Carlile‡ and L A Shuvalov§

† Joint Institute for Nuclear Research, 141980 Dubna, USSR

‡ Rutherford Appleton Laboratory, Chilton, Oxon. OX11 0QX, UK

§ Institute of Crystallography, Academy of Sciences of USSR, 117333 Moscow, USSR

Received 29 January 1991, in final form 28 August 1991

Abstract. The diffusion of protons in the superionic phase of $CsHSO_4$ was investigated by quasielastic neutron scattering (QNS) on the IRIS spectrometer at the pulsed spallation neutron source ISIS, Rutherford Appleton Laboratory, UK. Two processes with different characteristic times could be distinguished: long-range translational diffusion with a diffusion coefficient $D = (1.00\text{–}1.17) \times 10^{-7}$ cm^2 s^{-1} (for a temperature range from 423 to 448 K) and jump rotation of HSO_4 groups between two possible orientations, the corresponding non-equivalent proton sites being 2.3 Å apart.

1. Introduction

Caesium hydrogen sulphate ($CsHSO_4$) (CHS) was the first crystal in the $MeXAO_4$ family of compounds (where Me ≡ Cs, Rb; X ≡ H, D; A ≡ S, Se) which was observed to undergo a phase transition to a superionic state (Baranov *et al* 1982). The first-order phase transition at $T_c = 414$ K is accompanied by a sharp increase in conductivity to $10^{-2}\ \Omega^{-1}$ cm^{-1}. According to NMR measurements (Blinc *et al* 1984) and earlier neutron experiments (Belushkin *et al* 1987, 1991), the main contribution to the enhanced conductivity stems from the mobility of protons.

The phase diagram for CHS is (Belushkin *et al* 1987)

$$\underset{P2_1/c}{\text{phase III}} \xrightarrow{330\text{–}370\,\text{K}} \underset{P2_1/c}{\text{phase II}} \xrightarrow{414\,\text{K}} \underset{I4_1/amd.}{\text{phase I}}$$

Crystallographic aspects of the proton transport have been measured by high-resolution powder diffraction experiments (Belushkin *et al* 1991). In the low-conductivity phases III and II the number of protons per unit cell is equal to the number of positions for them. Hydrogen bonds link SO_4 tetrahedra so as to form zigzag chains. Hydrogen atoms are localized on the bonds and their mobility is low. The superionic phase I has tetragonal symmetry (space group, $I4_1/amd$) with four formula units per unit cell as shown in figure 1. From the structural data it turns out that the number of protons in a unit cell is six times lower than the number of available positions. The hydrogen atoms randomly occupy the 16f and 8e crystallographic positions with the probability ratio $p(16f)/p(8e) = 0.38$. It is approximately 2.5 times more probable to find hydrogen in the 16f position than in the 8e one. This is the underlying structural reason for the high mobility of

0953-8984/92/020389 + 10 $04.50 © 1992 IOP Publishing Ltd

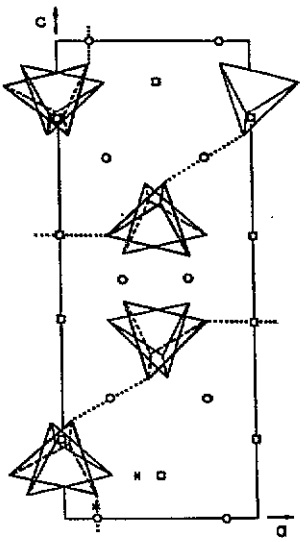

Figure 1. The crystal structure of the CHS superionic phase as projected on the a–c crystal plane according to Belushkin *et al* (1991). Only oxygen and hydrogen positions are marked for clarity. One of the possible hydrogen binding schemes is shown. The bold tetrahedron represents one of the four SO_4 group orientations and the thin tetrahedron shows the other. Each oxygen position is doubled along the b axis. Open circles represent 16f hydrogen positions and open squares 8e hydrogen positions. The asterisk shows one well of the double-minimum potential for the proton in the hydrogen bond (see section 3.3).

protons. Proton hopping and jump rotation of HSO_4 groups were inferred from the crystallographic studies. The existence of HSO_4 rotations also follows from the optical spectroscopy data (Pham-Thi *et al* 1985, 1987, Dmitriev *et al* 1986). The mechanism for the proton transport in CHS, suggested on the basis of the NMR experiment (Blinc *et al* 1984), also involves a hindered HSO_4 rotation followed by a subsequent proton translation. This concept was confirmed in the previous quasielastic neutron scattering (QNS) measurements (Colomban *et al* 1987), although translational diffusion was examined at low-momentum transfer only (within the hydrodynamic regime), and no model fitting was attempted to describe the HSO_4 rotation.

Our aim was to study quasielastic scattering over a wide range of momentum transfers using different spectrometer resolutions to identify translational and rotational processes and to give a model description of diffusion on the basis of our earlier structural work (Belushkin *et al* 1991).

2. Experimental details

The powder sample was produced as described previously (Belushkin *et al* 1987), dried in air and placed in a sealed slab-shaped aluminium container 40 mm × 40 mm square and 1 mm thick. The temperature of the sample was maintained with an accuracy of 1 K.

Neutron scattering experiments were carried out using the IRIS high-resolution inelastic scattering spectrometer, at the ISIS pulsed spallation neutron source, at the Rutherford Appleton Laboratory (UK). The incident neutron pulse covers a wide energy range, the neutron energy being determined by time of flight from the moderator to the sample, whilst the scattered neutron energy was selected by pyrolytic graphite crystal analysers in near-back-scattering geometry, which provided the parameters given in table 1. The IRIS spectrometer is capable of collecting 51 QNS spectra simultaneously, at scattering angles from 15° to 165°, thereby scanning a wide range of momentum transfer.

Table 1. Parameters for QNS.

Reflecting crystal plane	Energy resolution (μeV)	Q-range (momentum transfer) ($Å^{-1}$)
002	15	0.27–1.78
004	50	0.54–3.55

QNS spectra were collected at five temperatures: 403 K ($T < T_c$) and 423, 433, 443 and 448 K ($T > T_c$). The experimental data were normalized to the incident spectrum calibrated with reference to the scattering from vanadium.

The spectrometer resolution profile was defined by fitting an analytical function to the vanadium data. For the (002) graphite reflection a Gaussian function convoluted with an exponential decay plus a second underlying broad Gaussian gave a good fit to the experimental data. For the (004) graphite reflection a summation of two half Lorentzian functions knotted at the centre of the elastic line are a good description. Analytically generated functions make the quasielastic fitting processes described in section 3 below much more straightforward. The quality of the fits are illustrated in figure 2.

For a material with several phase transitions such as CHS it is very important to monitor the crystallographic phase simultaneously with the QNS measurements because of the strong influence on the phase diagram of the type of treatment undergone by the sample (Baranowski *et al* 1986, Belushkin *et al* 1987). The IRIS spectrometer is equipped with an array of diffraction detectors at scattering angles close to 170° with a resolution in $\Delta d/d$ of 2.5×10^{-3} that served this purpose. In figure 3 the neutron diffraction patterns for three temperatures are shown. These patterns are characteristic of a freshly prepared CHS sample and confirm that the quasielastic scattering spectra were taken in the correct phases.

3. Results and discussion

3.1. Translational proton diffusion

The translational diffusion was studied with high resolution (15 μeV; 002 graphite plane). The quasielastic line shape for the superionic phase I of CHS was accurately described by a single Lorentzian function, convoluted with the instrument resolution function, plus a background term (figure 4). Spectra corresponding to certain Q-values had to be excluded owing to contamination with coherent scattering (diffraction). This contamination was determined by mapping onto the inelastic detectors the diffraction patterns shown in figure 3. The dependence of the quasielastic intensity on Q^2 for $T =$ 423, 433, 443 and 448 K is shown in figure 5. It is linear on a logarithmic scale, in accordance with the general formula for the incoherent scattering law (Bee 1988, p 67):

$$S_{\text{inc}}(Q, \omega) = \exp(-\langle u^2 \rangle Q^2)[S^{\text{R}}_{\text{inc}}(Q, \omega) + S^{\text{I}}_{\text{inc}}(Q, \omega)] \quad (1)$$

where $\langle u^2 \rangle$ is the mean square displacement which enters into the definition of the Debye–Waller factor:

$$2W = \langle u^2 \rangle Q^2. \quad (2)$$

The mean square displacements as determined from the slopes of the lines in figure 5 are shown in figure 6 as a function of temperature; there is a clear linear dependence.

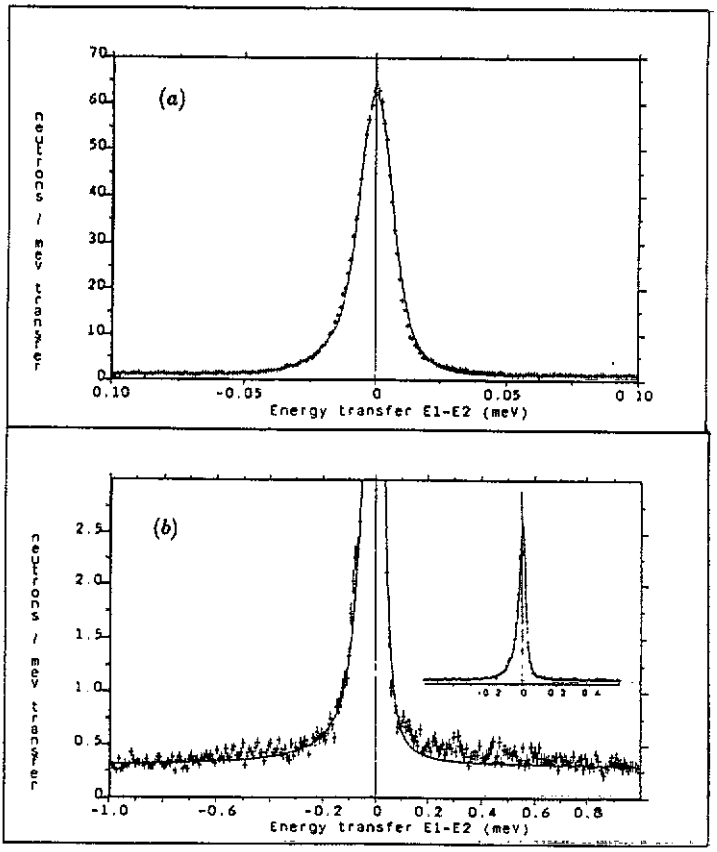

Figure 2. A fit of the vanadium data by analytical resolution functions as described in the text: (*a*) (002) graphite reflection, corresponding (FWHM) resolution is 15 μeV; (*b*) (004) graphite reflection, corresponding (FWHM) resolution is 50 μeV.

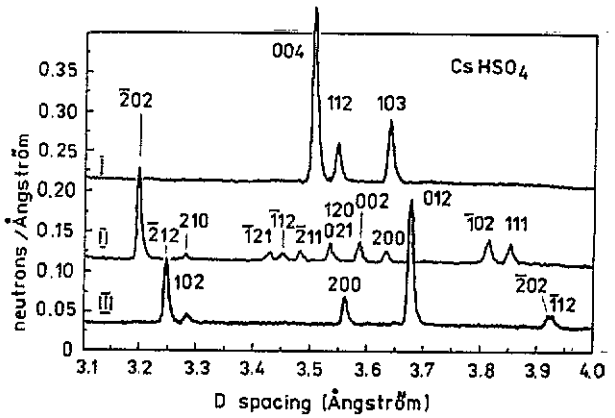

Figure 3. Neutron diffraction spectra from CHS obtained simultaneously with the quasielastic data at 293 K, 403 K and 433 K, corresponding to the three phases III, II and I respectively of the sample.

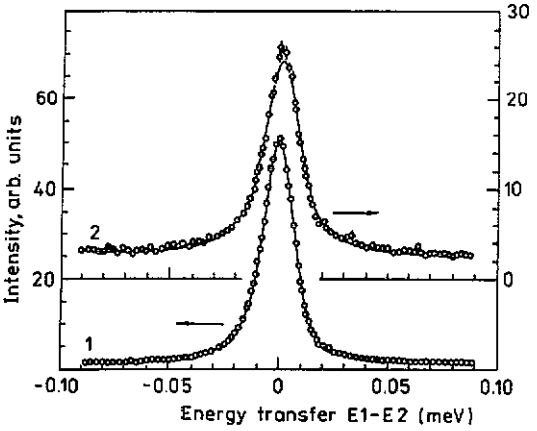

Figure 4. Example of quasielastic spectra obtained with a resolution of 15 μeV for Q-values of 0.6 and 1.78 $Å^{-1}$: ○, experimental data at 443 K; ——, Lorentzian convoluted with the resolution, plus background.

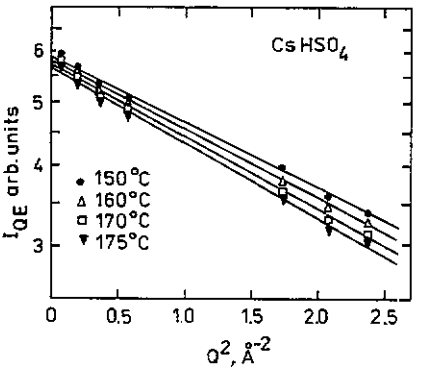

Figure 5. The dependence of the quasielastic intensity (on a logarithmic scale) on the momentum transfer squared: ●, △, □, ▼, experimental data; ——, best fit using the formula $I \propto \exp(-Q^2\langle u^2\rangle)$ (see equations (1) and (2)).

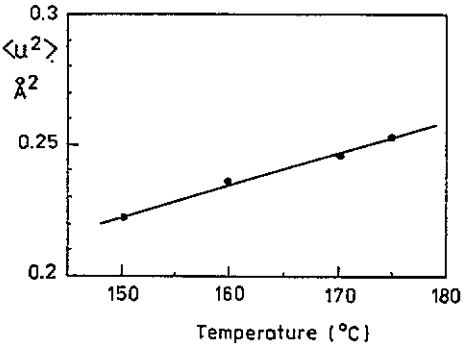

Figure 6. The temperature dependence of the mean square displacements of the protons in the hydrogen bonds.

A further analysis of the jump diffusion of the CHS protons was performed within the framework of the Chudley–Elliott model. This model has been deliberately chosen to determine a first approximation to the proton jump dynamics even though its assumptions are somewhat violated by the fact that the proton positions are unequally populated.

The rate equation for the probability $P(r, t)$ of finding an atom on a site at a distance r from an arbitrarily chosen origin is (Bee 1988, p 157)

$$\frac{\partial}{\partial t} P(r, t) = \frac{1}{n\tau} \sum_{l_i} [P(r + l_i, t) - P(r, t)] \tag{3}$$

where the summation is performed over n vectors l_i from the atom site to that of its

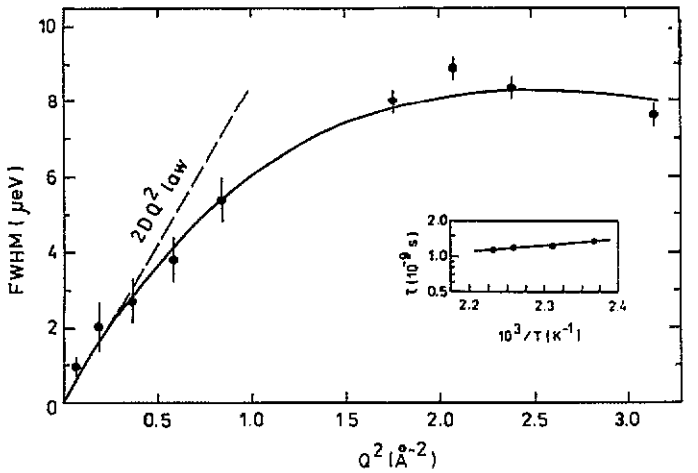

Figure 7. The dependence of the Lorentzian FWHM versus Q^2 at $T = 433$ K (note that equation (5) corresponds to the HWHM): ●, experimental data; ——, best fit to the data using the Chudley–Elliott model; – – –, Fick's law with a diffusion coefficient obtained from previous NMR results (Blinc *et al* 1984). The inset shows the temperature dependence of the correlation times for translational jump diffusion of the protons.

nearest neighbours. The jump rate is assumed to be the same for all neighbours. The scattering law can then be obtained, following the standard procedure:

$$S_{\text{inc}}(Q, \omega) = (1/\pi)[\Delta\omega(Q)/\{[\Delta\omega(Q)]^2 + \omega^2\}]. \tag{4}$$

We have used the isotropic approximation to analyse the data and, in this case, the averaging of $\Delta\omega(Q)$ over 4π gives for the quasielastic width (Lorentzian half-width at half-maximum (HWHM))

$$\Delta\omega(Q) = (1/\tau)\{1 - [\sin(Ql)]/Ql\}. \tag{5}$$

Equation (5) fits the dependence of the Lorentzian width on the momentum transfer fairly well (figure 7). The resultant proton jump length is 2.8 Å, in good agreement with the mean distance between 16f and 8e lattice positions, as derived from the structural data (Belushkin *et al* 1991). The dependence of the proton jump times τ plotted on a logarithmic scale against inverse temperature is shown in the inset to figure 7.

The Arrhenius formula

$$\tau = \tau_0 \exp(E_a/kT) \tag{6}$$

yields an activation energy E_a of (0.1 ± 0.03) eV for the proton hopping between the 16f and the 8e positions. The quasielastic scattering results can be compared with those from NMR (Blinc *et al* 1984) by means of the macroscopic diffusion coefficient. According to the formula $D = l^2/6\tau$ for the Chudley–Elliott model, for the temperatures from 423 to 448 K the diffusion coefficient varies between 1.00 and 1.17×10^{-7} cm^2 s^{-1}. Fick's law, with the diffusion coefficient extracted from the NMR data, is shown in figure 7 as a broken line, in good agreement with the present results.

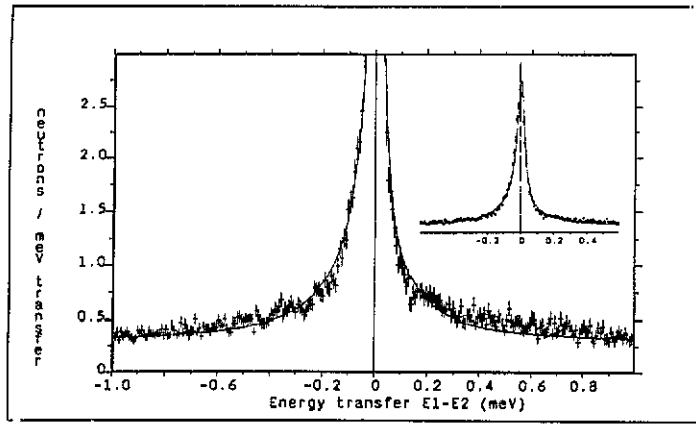

Figure 8. An example of a quasielastic spectrum obtained with a resolution of 50 μeV at Q = 1.83 $Å^{-1}$: ——, best fit using two Lorentzians, convolved with the resolution function, plus background.

3.2. Jump rotation of the HSO_4 groups

As well as translational jumps, the protons in the superionic phase of CHS can also be involved in a reorientation of the HSO_4 groups (Pham-Thi *et al* 1985, Dmitriev *et al* 1986, Colomban *et al* 1987). This process is faster than the translational process and needs the 50 μeV resolution option of the spectrometer to be successfully studied. Rotational diffusion produces a two-component spectrum containing a narrow translational line and a less intense broader line, resulting from reorientations of the HSO_4 group. When treated numerically by a convolution of two Lorentzian functions with the resolution function, the two components are difficult to resolve, and their parameters appear to be correlated. This obstacle was avoided to a certain extent by employing the information on the narrow Lorentzian extracted from the higher-resolution 15 μeV spectra. In the overlapping region of Q (0.54–1.78 $Å^{-1}$) of the (004) data and the (002) data, the width of the narrow Lorentzian could be fixed, and a refinement of the broader Lorentzian gave a width equal to 0.30 ± 0.08 meV, in agreement with the estimates of Colomban *et al* (1987). This value was then kept fixed in the further analysis of the full Q-range. An example of such a fit to the QNS data is shown in figure 8.

In view of what has been said above, no direct model fitting of various scattering laws was possible. One could, however, succeed in extracting an elastic incoherent structure factor (EISF) and compare it with the predictions of various models for the reorientation. The best results were obtained for a model of jump reorientation between two non-equivalent positions (see, e.g., Bee 1988, p 190, Krawczyk 1987). Following Bee (1988), one can introduce the probabilities τ_1 and τ_2 that a proton jumps from a 16f crystallographic site to an 8e site, and from the 8e site back to the 16f site in the $I4_1/amd$ superionic phase. The corresponding rate equations are

$$(\mathrm{d}/\mathrm{d}t)p(r_1, t) = -(1/\tau_1)p(r_1, t) + (1/\tau_2)p(r_2, t) \tag{7a}$$

$$(\mathrm{d}/\mathrm{d}t)p(r_2, t) = (1/\tau_1)p(r_1, t) - (1/\tau_2)p(r_2, t) \tag{7b}$$

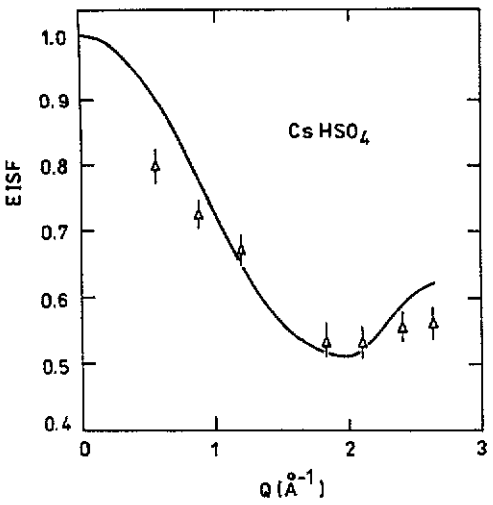

Figure 9. The EISF for jump reorientation of the HSO_4 groups: Δ, experimental values at 433 K; ——, best fit using equation (9).

where $p(r_1, t)$ and $p(r_2, t)$ are the probabilities of finding the proton at a time t at sites r_1 (16f) and r_2 (8e), respectively. This leads to the following scattering law:

$$S^{R}_{inc}(Q, \omega) = [1/(1+\rho)^2]\{[1 + \rho^2 + 2\rho j_0(Qd)]\delta(\omega) + (2\rho/\pi)[1 - j_0(Qd)]\,\Gamma/(\Gamma^2 + \omega^2)\} \tag{8}$$

where $\rho = \tau_1/\tau_2$, $j_0(Qd)$ is the zero-order spherical Bessel function, $d = |r_2 - r_1|$ is the jump distance between two sites and Γ is the HWHM of the Lorentzian function describing the quasielastic scattering. Then, from the definition of the EISF as the ratio of the purely elastic intensity to the total elastic plus quasielastic intensity,

$$\text{EISF} = [1 + \rho^2 + 2\rho j_0(Qd)]/(1+\rho)^2. \tag{9}$$

Note that in the case of a combination of translational and rotational diffusional components, for the purposes of the definition of the EISF, the translational component is taken to be purely elastic.

Equation (9) follows directly from (8) if one calculates the ratio of the first term in (8) integrated over ω (elastic intensity) to the total $S^{R}_{inc}(Q, \omega)$ also integrated over ω. The EISF is a measure of the time-averaged spatial distribution of the proton in lattice. It contains the most important geometrical information on proton dynamics.

In figure 9, the points show the experimentally derived EISF, and the full curve is the best fit using equation (9). The value obtained for the ratio ρ is 0.38, in excellent agreement with the 16f-to-8e occupancy ratio obtained for the structure (Belushkin *et al* 1991). The resultant distance d of 2.3 Å, however, is smaller than that between the 16f and 8e sites obtained both from the diffraction (2.7–2.9 Å) and from the translational diffusion results (2.8 Å). This issue will be covered in the following section in more detail.

3.3. The mechanism of proton diffusion in the superionic phase

The above results lead to a consistent picture of proton transport in the superionic phase of CHS.

Let us recall that the number of protons is six times smaller than the number of lattice sites that they occupy. Therefore, the protons can be considered to be disordered with respect to the network of possible hydrogen bonds that they can explore in the superionic phase. This network is subjected to a permanent building and rebuilding as the protons change their positions.

It has been established that the protons participate in two different translation processes, whose characteristics have been discussed in sections 3.1 and 3.2. Although the majority of these characteristics agree with the results of earlier experiments, others disagree. We have found an activation energy for proton hopping of 0.1 eV which is considerably lower than the value that the conductivity measurements give of 0.3 eV (Baranov *et al* 1982). According to the present results, the protons jump between positions 2.3 Å apart, while from the structural data the average distance between the 16f and 8e positions is 2.8 Å.

The discrepancy can be explained if one assumes that the hydrogen bond exhibits a double-minimum potential. In this case the elementary transport process would be a three-stage process. When the proton is localized at one minimum (shown by an asterisk in figure 1), it forms an HSO_4 group, and the weaker (and longer) part of the hydrogen bond can be easily broken. The HSO_4 group is now free to perform rotation around the sulphur atom. If there is no other SO_4 group in position to form a new hydrogen bond, then the previous configuration can be restored. This is a fast process, and it is observable only with the wider resolution at 50 μeV. Since the 16f and 8e crystallographic positions correspond to the centres of the lines connecting the oxygen atoms which participate in the hydrogen bond, the distance actually covered by a hopping proton would have to be shorter than the 16f and 8e static distance inferred from the crystallographic structure (see figure 1)†. If, on the other hand, after rotation a receptive SO_4 group could be found, then a new hydrogen bond would become established and the proton would move between the potential minima. A different HSO_4 group would then be formed, and the story would be repeated. The activation energy for the proton to move from one potential minimum to the second along a hydrogen bond and the activation energy for the proton transfer between different hydrogen bonds then define the activation energy for conductivity.

A simplified treatment of the proton long-range diffusion within the framework of the Chudley–Elliott model has yielded consistent results which are in good agreement with the structural data.

Acknowledgments

The authors wish to express their thanks to W Zajac and J Krawczyk for valuable discussions and for their help in data processing and J-C Lassegues for critical remarks and information about his experiments prior to publication. Thanks are also due to A Smith for experimental support. One of the authors (AVB) would like to thank the

† A further possibility of explaining the shorter jump distance was pointed out by J-C Lassegues (private communication, 1991). From structural data (Belushkin *et al* 1991), HSO_4 jumps between 16f–16f positions are also possible (a distance of 1.88 Å). The HSO_4 jumps between positions separated by different distances should lead to a multicomponent structure of the quasielastic line. Such a structure was observed in Lassegues' experiment. Our data do not permit us to carry out such a multicomponent analysis. Single Lorentzian fitting should nevertheless give a reliable mean value for the distance between 16f–8e (2.7–2.9 Å) and 16f–16f (1.88 Å) positions, which in fact is the case.

Science and Engineering Research Council and the Rutherford Appleton Laboratory for access to the ISIS facilities.

References

Baranov A I, Shuvalov L A and Schagina N M 1982 *JETP Lett.* **36** 459–62
Baranowski B, Friesel M and Lunden A 1986 *Z. Naturf.* a **41** 733–6
Bee M 1988 *Quasielastic Neutron Scattering* (Bristol: Adam Hilger) pp 189–94
Belushkin A V, Natkaniec I, Plakida N M, Shuvalov L A and Wasicki J 1987 *J. Phys. C: Solid State Phys.* **20** 671–87
Belushkin A V, Shuvalov L A, David W I F and Ibberson R M 1991 *Acta Crystallogr.* B **47** 161–6
Blinc R, Dolinsek J, Lahajnar G, Zupancic I, Shuvalov L A and Baranov A I 1984 *Phys. Status Solidi* b **123** K83–7
Colomban Ph, Lassegues J C, Novak A, Pham-Thi M and Poinsignon C 1987 *Dynamics of Molecular Crystals* (Amsterdam: Elsevier) pp 269–75
Dmitriev V P, Loshkarev V V, Rabkin L M, Shuvalov L A and Yuzyuk Yu I 1986 *Kristallografia (USSR)* **31** 1138–44 (in Russian)
Krawczyk J 1987 *Acta Phys. Pol.* A **71** 953–7
Pham-Thi M, Colomban Ph, Novak A and Blinc R 1985 *Solid State Commun.* **55** 265–70
—— 1987 *J. Raman Spectrosc.* **18** 185–94